AE International – Asia

Atmospheric Environment 38 (2004) 6239–6252

ATMOSPHERIC ENVIRONMENT

www.elsevier.com/locate/atmosenv

Identification and characterization of sources of atmospheric mineral dust in East Asia

Jie Xuan[a,*], Irina N. Sokolik[b], Jingfu Hao[c], Fahui Guo[c], Hengqing Mao[c], Guiming Yang[c]

[a]*Environment Science Center, Peking University, Beijing 100871, China*
[b]*School of Earth and Atmospheric Sciences, Georgia Institute of Technology, Atlanta, USA*
[c]*National Meteorological Center, China Meteorological Administration, Beijing, China*

Received 26 January 2004; received in revised form 9 June 2004; accepted 18 June 2004

Abstract

The dust source region in East Asia consists of deserts and gobi-deserts in Northern China and Southern Mongolia. First part of this paper discusses the identification criteria of dust sources. A dust emission mechanism serves as the basis of our analyses and the dust storm frequency is considered the principal criterion. The second part studies Mongolian dust sources. Three types of dust sources in Southern Mongolia are identified and characterized, whose dust emission rates are calculated with US EPA (Environmental Protection Agency) formulas. The dust emission rate increases from north to south across the country by five orders with the strongest dust emission area in the south gobi-area. The third part reveals that the united dust source region in East Asia is comprised of two parts or systems: (a) the Mongolian Plateau dust source system, and (b) the Tarim Basin dust source system. The two systems are related and distinguished not only by topography and the distribution pattern of gobis, deserts and loess lands, but also by soil texture, climate, and dust storm meteorology. For example, M (moving) type dust storms are typical for the Mongolian Plateau system while S (stationary) type dust storms are typical for the Tarim Basin system. Total dust emission from the source region in East Asia is estimated at 10.4×10^6 ton yr^{-1} for PM_{10} (dust particles smaller than 10 μm in diameter), 27.6×10^6 ton yr^{-1} for PM_{30}, and 51.3×10^6 ton yr^{-1} for PM_{50}.

Keywords: Atmospheric dust; Dust sources; Source identification criteria; Mongolia; East Asia

1. Introduction

It is essential to identify dust sources and estimate their emission strengths in the research of atmospheric dust. The following geographic elements have been taken as main source characters (indicators), some of which are soil and meteorological conditions while the others are observed dust indicators. The former includes: the soil moisture content (Joussaume, 1990), the vegetation coverage (Mahowald et al., 1999), the soil texture (Tegen and Fung, 1994), the surface roughness (Marticorena and Bergametti, 1995), the 'binding energy' which represents cohesion forces between soil particles (Shao et al., 1993), and the topographic features (Ginoux et al., 2001; Zender and Newman, 2002). The latter includes: the dust storm frequency based on visibility observation (Littmann, 1991;

*Corresponding author. Tel./fax: +86-10-6287-1784.
E-mail address: jiexuan@pku.edu.cn (J. Xuan).

1352-2310/$ - see front matter © 2004 Elsevier Ltd. All rights reserved.
doi:10.1016/j.atmosenv.2004.06.042

Middleton, 1991), a satellite image product: Total Ozone Mapping Spectrometer, Absorbing Aerosol Index (TOMS AI) (Goudie and Middleton, 2001; Prospero et al., 2002). Also, the dust emission rate has been calculated to characterize dust sources (Xuan, 1999; Xuan et al., 2000; Xuan and Sokolik, 2002). It seems that no single factor can serve as the unique criterion for dust sources, so multidisciplinary analysis is necessary. The principles of our multidisciplinary analysis are concluded to be a set of identification criteria.

Deserts and gobi-deserts in Southern Mongolia and Northern China form a united dust source region in East Asia. We have classified Chinese dust sources into three types (Xuan and Sokolik, 2002): Type 1: deserts in dry agricultural areas, Type 2: deserts and gobi-deserts on flat plateaus, and Type 3: deserts and gobi-deserts in topographical lows. The three types are also found in Southern Mongolia. Mongolian sources are characterized and the dust emission rates are calculated with US EPA models.

Our conclusions in studying dust sources in both countries suggest that the dust source region in East Asia consists of two parts or systems which have commonalities and differences in palaeogeography, topography, morphology (distribution pattern of deserts, gobis, with or without loess lands), soil texture, climate, and especially, dust storm meteorology.

2. Identification criteria of dust sources

Xuan and Sokolik (2002) proposed a set of key source factors, which reflects the general characteristics of dust sources. It was further improved by studying Mongolian sources. The dust emission mechanism serves as the basis for our analyses, the dust storm frequency is considered the principal source criterion, and the dust emission rate quantifies the 'source strength'. TOMS AI is important in general but not included in our criterion set because it obviously underestimates dust sources in East Asia.

2.1. Dust emission mechanism

With some exceptions, e.g., dust emission without particle saltation (Zobec et al., 2003) and the vortex lifting mechanism (Iversen, 2002), it is well recognized that dust emission is controlled by saltating sand particles which convey momentum of the wind flow to, and cast out, the finest dust particles lying in the bed (Bagnold, 1941; Alfaro et al., 2003). Also, the dust emission rate is supposed to be proportional to the horizontal flux of saltating particles (Gillette, 1979). The dust emission mechanism is now simply expressed as: "a factor that favors sand saltation favors dust emission; and, the stronger the saltation, the stronger the surface emission of dust into the air."

2.2. General discussion of key source factors

2.2.1. Annual mean dust storm frequency

As direct evidence of strong dust emission, a dust storm is defined by horizontal visibility worse than 1 km. Dust storm frequency is the principal source indicator. Because there are few weather stations located in desolate areas like deserts, and since a strong dust storm can travel over long distance, a dust source region exists inside a high dust storm frequency region and close to its upwind border. It is suggested that an annual mean dust storm frequency of $>5\,\mathrm{day\,yr^{-1}}$ indicates dust sources, and $>20\,\mathrm{day\,yr^{-1}}$ for strong dust sources.

2.2.2. Annual mean wind speed

The dust emission rate strongly depends on the annual mean wind speed, or the time percentage of wind speed higher than a threshold of, say, $5.4\,\mathrm{m\,s^{-1}}$ in a year.

2.2.3. Annual mean aridity, precipitation, and vegetation coverage

Representing the water budget of the surface soil, the aridity R is defined as the ratio of maximum potential evaporation (evapotranspiration) e^* over precipitation p:

$$R = \frac{e^*}{p}. \tag{1}$$

The maximum potential evaporation e^* is calculated by every-day air temperature. According to Chao (1984), $R<1$ defines a wet area, $1<R<2$ for a transition area, $R>2$ for an arid area, and, especially, $R>4$ for deserts and gobi-deserts. It is suggested that an annual mean aridity of $R>2.5$ and a precipitation of $p<300\,\mathrm{mm\,yr^{-1}}$ are indicative of dust sources.

Vegetation coverage agrees well with the distribution of the precipitation and the aridity. In deserts and gobi-deserts, which serve as the main dust sources in East Asia, few plants can survive. The vegetation coverage is not included in our criterion set.

2.2.4. Surface soil texture, morphology, and topography

The dust emission mechanism suggests that soils in dust emitting surfaces must be rich in sand content so as to provide an abundance of loose, middle-sized particles for saltation. On the other hand, silt and clay are in the same size range of dust ($d<50\,\mu\mathrm{m}$) so that the Loess Plateau in Northern China was once considered a main dust source. However, the rich clay content, e.g., >20%, creates soil aggregates and clods so as to effectively depress sand saltation as well as dust emission (Amante-Orozco and zobeck, 2002). Also, severe soil aeolian erosion occurs only where surface soil is poor in both silt and clay contents, e.g., clay content lower than 5%

(Harpet et al., 2002). It is now suggested that, for dust sources, the surface soil is rich in sand content, say, $>50\%$, and poor in clay content, say, $<5\%$.

Many years of meteorological statistics for China show that most of the dust storms occur downwind of, and close to, the major deserts, and, the frequency of dust storms is higher nearer to the deserts (Xu and Hu, 1996). Moreover, the maximum dust storm frequency appears in oasis contained inside deserts. The extreme annual dust storm frequency is 37 day yr^{-1} in Minfeng (37°04′N, 82°43′E, an oasis in the south Taklimakan Desert), 34 day yr^{-1} in Minqin (38°38′N, 103°05′E, an oasis in the south Tengger Desert), and 36 day yr^{-1} in Ejinaqi (41°57′N, 101°04′E, an oasis in the south Central Gobi-desert) (Ding and Wang, 2001). It is suggested that desert and gobi-desert are both the right morphology of strong dust sources in East Asia.

The word 'gobi' means a stone-covered area, coming from the word 'govi' in Mongolian. Govi means a vast and flat area, where gobis, sand deserts, and dried clods are alternatively distributed, corresponding to the word 'gobi-desert' in English. Gobi-desert exists only in the aridest area of central Eurasia, i.e., Southern Mongolia and North-west China. Gravel covering the gobi surface can effect the dust emission both positively and negatively: gravel half-buried in sand (soil) surfaces decreases the effective wind shear force on the soil surface, resulting in stress partitioning (Nickling and Gillies, 2003), and a complete stony armor strongly depresses the aeolian motion of particles (Yi et al., 2002). On the other hand, it deforms the flow field close to the ground so as to promote sand saltation and consequent dust emission (Gillette, 1983). In reality, precipitation is rare in the gobi area, less than 50 mm yr^{-1} (Zhao, 1994), and is limited to the summer season so that the gobi surface becomes extremely dry in spring when the strong wind behind a cold front periodically blows through East Asia and is enhanced over the vast and flat gobi surface. As the surface wind speed often reaches 24–30 m s^{-1}, or even higher, on the south Mongolian Plateau (Qian et al., 1997), strong dust storms occur in spite of the gravel armoring and the below 0°C air temperature. A sobering example is the statistics that a total of 32 dust storms were reported in East Asia during spring 2001, 18 of which originated in Mongolian gobi-deserts (CMA, 2002). On the other hand, in the Tarim Basin, topography limits the surface wind speed to be less strong than on the Mongolian Plateau, and the effect of surface gravel on gobi-deserts is to depress dust emission.

On the Loess Plateau, the content of silt and clay in the surface soil is more than 90% and the sand and gravel content is in totally lacking (Xiong and Li, 1990). Also, the annual mean precipitation is around 400 mm yr^{-1} and the aridity is in the range of $1<R<2$. Vast dry grasslands and dry farmlands are typical landscapes on the Loess Plateau where dense vegetation coverage effectively depresses dust emission and the dust storm frequency is much lower than upwind deserts and gobi-deserts. Sun et al. (2000, 2001) defined 'dust fall' by visibility worse than 10 km with the wind speed low downwind of the 'dust rise' region or dust sources. They found that the Loess Plateau is the center of a strong dust-fall region. Their chemical analysis of soil samples proves also that the Loess Plateau was formed by millions of years of dust deposition (Zhang, 1999). It is suggested that the Loess Plateau (dry grassland and dry farmland as well) does not belong to strong dust sources.

It was once suggested by previous authors that all dust sources should be located in topographical lows, e.g., sea basins or mountain flanks, so that their surfaces could receive sediments—silt, sand, and gravel—carried by outflows from the surrounding mountains. However, sea basins in palaeogeographical periods may have been turned into different modern topographic features by tectonic movements, e.g., the Tarim Basin vs the Mongolian Plateau. Modern topographic features are not included in our source criterion set.

2.2.5. Annual mean dust emission rate

The calculation of the dust emission rate is based on the following US EPA formulas (OAQPS, 1977; Cowherd et al., 1979):

$$Q_{30} = 0.2058 esf\,\mathrm{PE}^{-2}, \tag{2}$$

$$Q_{50} = e c_{50} CKLV, \tag{3}$$

where Q_{30} and Q_{50} denote the annual mean dust emission rates, in units of ton $ha^{-1}\,yr^{-1}$, respectively, for dust particulates PM_{30} and PM_{50}; f is the threshold wind speed ratio (i.e., time percentage when the mean wind speed u is higher than a threshold value of 5.4 m s^{-1}); C is the so-called 'climatic factor' defined as $C = 0.504u^3\ \mathrm{PE}^{-2}$, where u is the annual mean wind speed and PE is Thornthwaite's precipitation–evaporation index; K is the surface roughness factor, L is the unsheltered field width factor, and V is the vegetation cover factor; e is the erosion index of the soil type (ton $ha^{-1}\,yr^{-1}$); and the other two soil parameters, s and c_{50}, are weight percentages of particulates smaller than 75 μm and 50 μm, respectively. Based on the hypotheses of the log-normal size distribution of soil particles and the emission rate of dust particles in a certain size range being proportional to their weight percentage in the surface soil, a method to calculate Q_{10}, the emission rate for PM_{10}, with calculated Q_{30} and Q_{50} has been developed. It is suggested that the annual mean dust emission rate in dust source regions is higher than a critical value, e.g., $Q_{10} > 10^{-4}$ ton $ha^{-1}\,yr^{-1}$.

2.3. Criteria for identification of dust sources

A set of five criteria for identifying dust sources in East Asia is based on the mechanism of dust emission: 'A factor that favors sand saltation favors dust emission; and, the stronger the saltation, the stronger the surface emission of dust into the air'. The five criteria are: (i) annual mean dust storm frequency (say $>5\,\mathrm{day\,yr^{-1}}$); (ii) annual mean wind speed, or time percentage of wind speed higher than $5.4\,\mathrm{m\,s^{-1}}$ in a year; (iii) aridity (say >2.5), or annual mean precipitation (say $<300\,\mathrm{mm\,yr^{-1}}$); (iv) soil texture rich in sand content (say $>50\%$) and poor in clay content (say $<5\%$); and (v) annual dust emission rate (say $>10^{-4}\,\mathrm{ton\,ha^{-1}\,yr^{-1}}$ for PM_{10} emission).

3. Mongolian dust sources

3.1. General environment of Mongolia

Most of the Mongolian Plateau belongs to Mongolia except for a southern strip known as the Inner-Mongolia Plateau. The east part of the country is the East Mongolia Plain, consisting of southern deserts and northern dry grasslands. The north and west parts are mountains—the Chentij Mountains in the northeast, Hangaj Mountains in the northwest, and Altaj Mountains in the west. The south part of Mongolia is a vast and flat gobi area. And, between the south gobi area and the north mountain area, a central strip of dry grasslands stretches from west to east. Further, the Great Lake Basin is located between the Hangaj and Altaj Mountains. The south Mongolian gobis extend southwest, across the border with China, showing extremely desolate landscapes, where neither vegetation nor animals can survive because there is no surface or underground water at all.

Thousands of kilometers from the oceans and high above the sea level, the Mongolian climate is extremely dry, continental and cold. The East Asian Monsoon can hardly reach the southeast edge of the East Mongolian Plain because of the barrier of the Great Khingan Ranges, therefore Mongolia is in the driest center of Eurasia. The north mountain area receives moisture from the Arctic Ocean so it is a little wetter. The annual mean precipitation is about 300 mm $\mathrm{yr^{-1}}$ in the north mountain area and is $<50\,\mathrm{mm\,yr^{-1}}$ in the south gobi area. Eighty percent of the annual precipitation occurs from late May to early September, mostly in July and August. This makes spring the driest season. The extreme continentality means that all meteorological elements reflect a large scale of variation. For example, the difference between maximum and minimum air temperature can be as large as 30 °C in a given day or 90 °C in a given year (Murzayev, 1958). It is also normal in Mongolia that the annual precipitation varies greatly from year to year. For example, the precipitation in Sainshand (44°52′N, 110°09′E) was $83\,\mathrm{mm\,yr^{-1}}$ in 1963 but, in the next year, it went up to $248\,\mathrm{mm\,yr^{-1}}$ (CMA, 1970). Such a great interannual change in precipitation means that, in drought years, severe dust storms occur even in the north mountain area. At the end of winter season, the south Siberian anti-cyclone named the 'Siberian High' becomes unstable and, in the following spring months, breaks down several times so that a succession of frontal systems traverses the country from northwest to southeast, resulting in strong surface wind, which is further strengthened over the vast and flat gobi surface. Spring is the main dust storm season. Generally, the annual wind speed is $>5\,\mathrm{m\,s^{-1}}$ in the south gobi area and it decreases from south to north, down to $2\,\mathrm{m\,s^{-1}}$ in the north mountain area.

Due to the cold and dry climate, the weathering process is weak so that surface soils are coarse in texture and poor in humus. All kinds of soils have a gravel content of 2–10%, sand content of $>60\%$, and a rather low content of silt and clay (Table 1). There is a coarse-to-fine trend in particle sizes from northwest to southeast, along the spring prevailing wind. Also, distributed along the direction are gobis, deserts, and loess lands (the Loess Plateau in China), showing a good accordance with the process of particle mobilization, transportation, and deposition. This means that Mongolian sources are the most upwind 'origin' of Asian dust.

Generally, the annual dust storm frequency is $F_{\mathrm{dust}}<10\,\mathrm{day\,yr^{-1}}$ in the north mountain area, it increases from north to south to $F_{\mathrm{dust}}>30\,\mathrm{day\,yr^{-1}}$ in the south gobi area (Tuvdendorzh, 1974; Littmann, 1991; Middleton, 1991; Sun et al., 2001; Natsagdorj et al., 2003).

From north to south, along with the decrease in precipitation, vegetation cover varies from forests in the north mountain area to the central belt of dry grasslands, then to the extreme desolate south gobi-deserts where vegetation cover is $<10\%$ or even equal to zero (Murzayev, 1958). Generally, the natural environment of Southern Mongolia is worse than that of Northern China—there are more gobis but less deserts in Mongolia, the Mongolian climate is drier, colder, and more continental, and Mongolian soils are poorer in humus, containing a lot of gravel. The poor alpine ecosystem of Mongolia is fragile. In the 1950s, the exploration of dry grasslands for farming near Ulan Bator resulted in serious soil erosion and desertification (Murzayev, 1958). Because of the small population of Mongolia and its grazing economy, the anthropogenic environmental degradation seems to be less severe than in Inner Mongolia of China.

Table 1
Mongolian soils and corresponding American surface soil texture categories

Mangolian soil type[a]	Surface soil texture[b](%)				American soil texture category[c]
	Gravel : > 1 mm	Sand 1–0.05 mm	Coarse silt 0.05–0.01 mm	Fine silt and clay < 0.01 mm	
Mountain meadow soil and Partial-peat soil	No soil profile data provided				Loam?
Black mountain meadow black soil and Mountain peat soil	3	61	20	16	Sandy-clay loam
Gray forest soil and Mountain black soil	8	76	5	11	Loamy sand
Dark chestnut soil, Chestnut soil and Lowland dark meadow soil	4	60	12	24	Sandy loam
Chestnut soil and Light chestnut soil	5	84	5	6	Loamy sand
Chestnut soil and Dark chestnut soil	3	81	7	9	Loamy sand
Chestnut soil and Thin-layer brown soil	4	77	15	4	Loamy sand
Gobi brown soil	7	70	7	16	Loamy sand
Solonchak and Salinized soil	4	76	10	10	Sandy loam
Alkalized–salinized soil complex	7	64	9	20	Sandy loam
Solonetz and Alkalized soil	3	66	12	19	Sandy loam
Alkalized–salinized soil complex with cracked surface	—	15	3	82	Clay
Meadow soil and Meadow bog soils (salinized or carbonated)	No soil profile data provided				Loam?
Desert sand	4	90	2	4	Sand
Pine wood sandy soil	2	90	8	—	Sand
Grassy sandy soil or Strong sandy area	10	85	1	4	Sand

[a]Pisparov (1959).
[b]Concluded from soil profiles of Pisparov (1959).
[c]Gillette (1979).

3.2. Aridity and dust emission rate of Mongolia

3.2.1. Calculation methods

With Eqs. (2) and (3), we calculated the dust emission rates Q_{10}, Q_{30}, and Q_{50}, as well as the aridity R, at 39 grid points in Mongolia, which are $2.5^\circ \times 2.5^\circ$ apart except for those close to the border (see the grid points in Fig. 1). Please see Xuan (1999), Xuan et al. (2000), and Xuan and Sokolik (2002) for details of the calculation methodology. The limited data availability requires specific data pre-processing, part of which is different from previous calculations for Chinese sources and described as follows.

The Mongolian climate data of 1937–1970 by Gonggerdaxi (1977) were used for the calculation. Neither daily air temperature nor annual mean evaporation data are available to calculate Thornthwaite's precipitation-evaporation index PE. As accurate Chinese climate data are available, we selected 10 grid points located on the Chinese side and as close as possible to the Mongolian border to obtain following regression relationship between the annual mean evaporation E ($\mathrm{mm\,yr^{-1}}$) and the monthly mean air temperature of July T_7 (°C):

$$\mathrm{E} = 333T_7 - 4750, \tag{4}$$

The relationship was then used to estimate the evaporation E in Mongolia with the corresponding T_7 data. Finally, the quantity PE was calculated with an empirical formula, which we developed in a previous study for Chinese sources (Xuan, 1999):

$$\mathrm{PE} = 300\frac{p}{E}. \tag{5}$$

For estimating the aridity R in Mongolia, we again analyzed the correlation between PE and R at the 10 grid points on Chinese side so as to obtain regression formula

$$R = \frac{152}{PE} - 2. \tag{6}$$

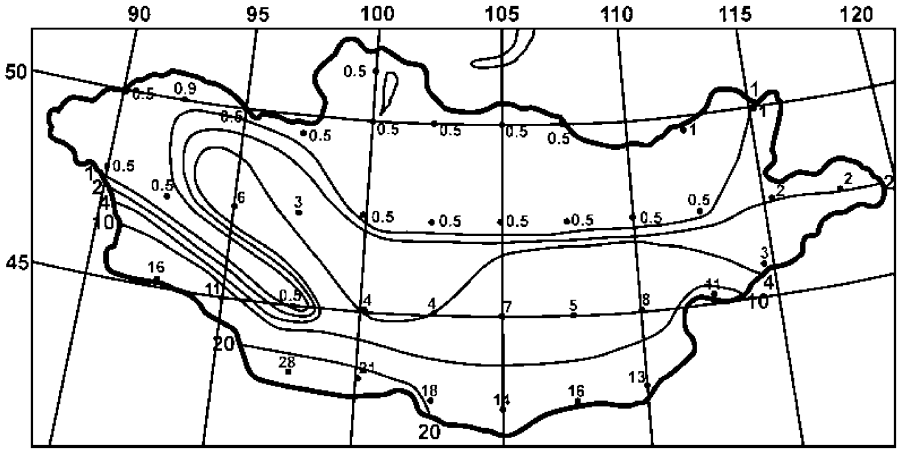

Fig. 1. Annual mean aridity of Mongolia.

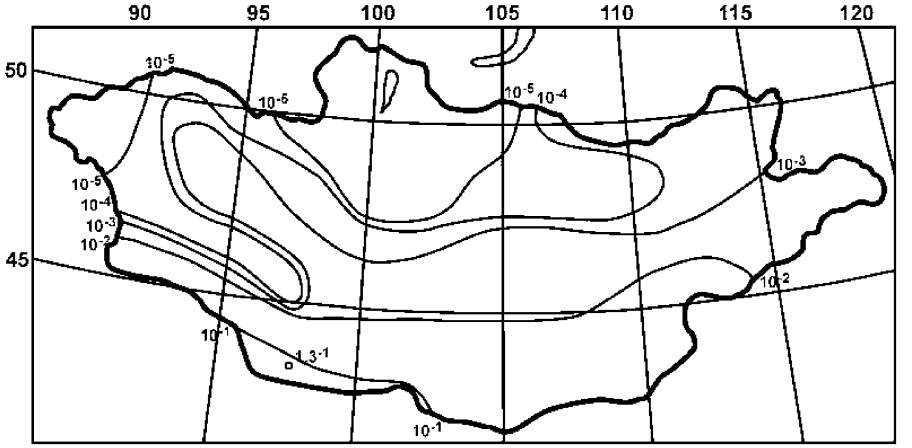

Fig. 2. Dust (PM_{10}) emission rate in Mongolia, ton ha^{-1} yr^{-1}.

Pisparov's (1959) soil profile data were used to estimate the surface soil texture, i.e., percentage content of gravel, sand, silt, and clay of the top 0–5 cm of the soil. With such estimated surface soil texture data, each of the 16 Mongolian soil types was identified with its corresponding American soil texture category (the soil texture triangle of Gillette, 1979). Please see Table 1. The three input soil parameters—e, s and c_{50}—were then evaluated with the American soil texture category (Jutze and Axetell, 1976).

3.2.2. Calculation results and analyses

Figs. 1–4 are the resultant contour maps of the aridity R and the dust emission rates Q_{10}, Q_{30}, and Q_{50}, respectively. In Fig. 1, north of the contour $R = 1$ is the north mountain area where the climate is a little wet ($R < 1$). The aridity R rapidly increases as one moves southward. South of the contour $R = 2$ are all deserts and gobis, and the contour $R = 4$ draws roughly the north border of the south gobi area. Further south, in a belt along the border with China, the aridity $R > 10$ with a maximum $R = 28$ appears in Outer Altaj Govi. The distribution of the aridity agrees very well with that of the annual precipitation and the dust storm frequency. In the region of $R > 2$, the precipitation is $p < 250$ mm yr^{-1} in the east part and < 150 mm yr^{-1} in the west part, and it rapidly decreases southward, down to < 50 mm yr^{-1} in the south gobi area (Gonggerdaxi, 1977). Also, the contours $R = 1$, 2, and 4 respectively coincide with the contours of the dust storm frequency $F_{dust} = 10$, 20, and 30 day yr^{-1} in Fig. 2 of Middleton (1991). Moreover, the contour $R = 2$ coincides well with the contour of the PM_{10} emission rate $Q_{10} = 10^{-3}$ ton ha^{-1} yr^{-1} in Fig. 2. Figs. 2–4 show similar distribution pattern of the dust emission rate: it is relatively low in the north mountain area but rapidly

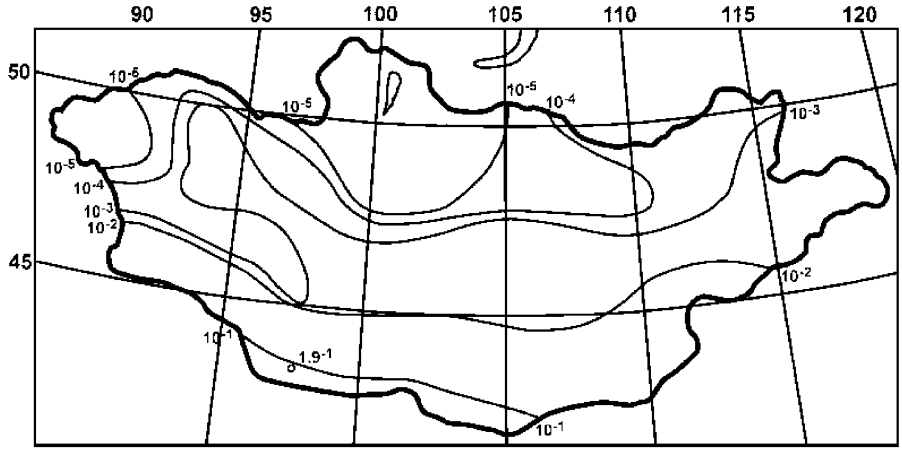

Fig. 3. Dust (PM_{30}) emission rate in Mongolia, ton ha^{-1} yr^{-1}.

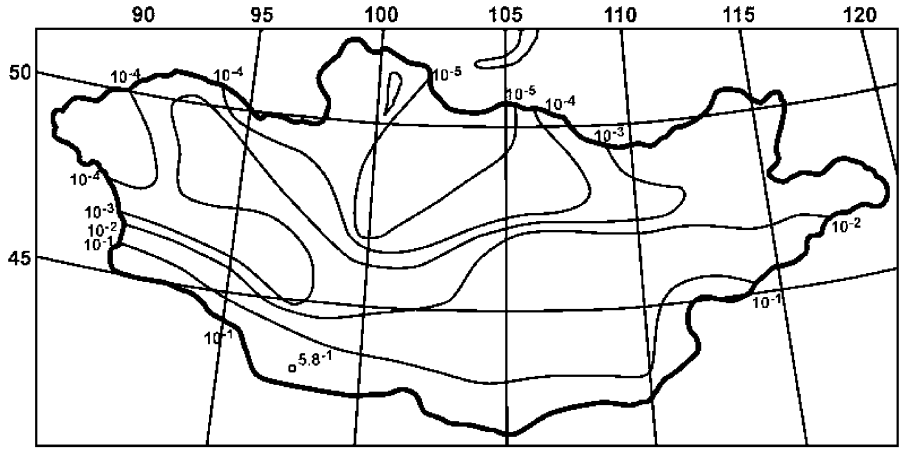

Fig. 4. Dust (PM_{50}) emission rate in Mongolia, ton ha^{-1} yr^{-1}.

increased from north to south by five orders. The maximum of the emission rates appears in Outer Altaj Govi, at the same place of the maximum aridity, equaling 1.3×10^{-1} ton ha^{-1} yr^{-1} for PM_{10}, 1.9×10^{-1} ton ha^{-1} yr^{-1} for PM_{30}, and 5.8×10^{-1} ton ha^{-1} yr^{-1} for PM_{50}. We estimated the total dust emission from Mongolian sources to be 2.0 million tons per year for PM_{10}, 2.9 million tons for PM_{30}, and 8.7 million tons for PM_{50}. It is suggested that Southern Mongolia is an important dust source region. In the source region, roughly, the annual precipitation is $p < 200$ mm yr^{-1}, the aridity $R > 2$, the dust storm frequency $F_{dust} > 20$ day yr^{-1}, and the dust (PM_{10}) emission rate $Q^{10} > 10^{-3}$ ton ha^{-1} yr^{-1}. It is interesting to notice that the maximum dust storm frequency in Middleton's Fig. 2 is east (downwind) of the maximum dust emission rates, showing an eastward transportation of the dust.

3.3. Three types of dust sources in Southern Mongolia

Like in China, dust sources in Mongolia are also classified into three types: (i) Type 1: deserts in dry agricultural areas, i.e., Omhang and Morzhuok Deserts in the south part of the East Mongolia Plain; (ii) Type 2: deserts and gobi-deserts on flat plateaus, i.e., the south gobi area covering three provinces—Dornogovi, Omnogovi and Dundgovi—and the south part of two other provinces—Bajanchongor and Govi-Altaj; and (iii) Type 3: deserts and gobi-deserts in topographical lows, i.e., Great Lake Basin. Fig. 5 shows both Mongolian and Chinese sources of the three types. Roughly, Type 1, 2, and 3 sources lie from east to west, along with decreasing precipitation and increasing aridity. No great difference has been found between sources of the same type that are in the two different countries. Type 2 sources in Mongolia contribute 97% of the total annual

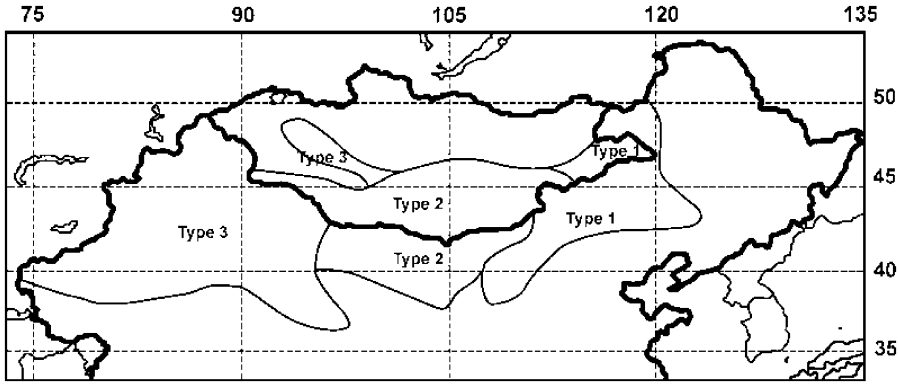

Fig. 5. Three types of dust sources in Southern Mongolia and Northern China.

dust emission, while, in China, most of the contribution comes from Type 3 sources. Table 2 is a brief characterization and comparison of the three types of dust sources in Mongolia and China.

4. Dust sources in East Asia

4.1. Two types of dust storms and two dust source systems

Combining our knowledge of Mongolian and Chinese sources, the dust source region in East Asia has been studied as a unity. Defined by horizontal visibility worse than 10 km, Fig. 6 shows the total dusty days F_d in spring (March–May) of three years, 2000–2002, in the area. It is interesting to see that the strong dusty area of $F_d > 10$ days is virtually divided into two parts, both having a strongest center of $F_d > 100$ days, i.e., the Taklimakan Desert in the Tarim Basin and the gobi area on the Mongolian Plateau. Chen and Chen (1987) classified dust storms in East Asia into four types, among which the S (stationary) type and M (moving) type are basic ones. 80% of their S type dust storms occurred over the Taklimakan Desert and vicinity, while 70% of the M type originated over the gobi area and desert area of 90–105°E, i.e., the Mongolian Plateau and its southern extension. As an example, the surface wind vector field and the horizontal visibility in Fig. 7 show both S type dust storms over the Taklimakan Desert and M type dust storms over the Mongolian Plateau and downwind areas. And, the latter are moving southeast.

It is suggested that the source region in East Asia consists of two parts or systems: (i) the Mongolian Plateau dust source system, including deserts and gobi-deserts on the Mongolian Plateau and its southern extension—the Ordos Plateau and Alxa Plateau; and (ii) the Tarim Basin dust source system, including deserts and gobi-deserts in the Tarim Basin, Junggar Basin, and eastern vicinity.

4.2. Palaeogeography and modern topography of the two dust source systems

At the beginning of the Palaeozoic Era, the Cambrian, some 570 million years ago, the area of the two systems was under seawater. By the end of the era, late Permian, some 250 million years ago, the sea bottoms had started to lift by tectonic movements, gradually becoming land surfaces. In the early Quaternary Period, early Pleistocene, some 2.5 million years ago, the bottom of the Old Gobi Basin and Old Ordos Basin had become the flat terrestrial surface of the modern Mongolian Plateau of 1500 m above sea level. And, southwest of the plateau, the bottom of the Old Tarim Basin and Old Junggar Basin had also lifted to 1000 m elevation but still remained lower than the surrounding topography. The modern Tarim Basin and Junggar Basin are surrounded by the Altaj Mountains in the north, Tainshan Mountains in between, Tibetan Plateau in the south, Pumir Plateau in the west, and Mongolian Plateau and Kunlun Mountains in the east (Liao, 1999).

4.3. Morphology, soil texture, and climate of the two dust source systems

The morphologic distribution of deserts and gobi-deserts shows different patterns for the two systems. In the Mongolian Plateau system, distributed from northwest to southeast are Mongolian gobis followed by Chinese deserts. Further southeast, out of the system, lies the huge Loess Plateau. As the spring prevailing wind blows southeast, the morphologic distribution order corresponds to the process of particle mobilization, transportation and deposition. Contrary to the 'linear (aeolian) distribution pattern' of the Mongolian Plateau system, the morphologic distribution in the

Table 2
Three types of dust sources in Southern Mongolia and Northern China

Category	Type 1			Type 2			Type 3		
Topography (elevation above sea level)[a,b]	Plain and plateau (500–1500 m)			Flat plateau (1000–1800 m)			Basin (300–1200 m)		
Morphology[a,b]	Deserts			Deserts and gobi-deserts			Deserts and gobi-deserts		
Area (km^2)	12.3×10^4 (Mongolia)			59.4×10^4 (Mongolia)			12.3×10^4 (Mongolia)		
	78.7×10^4 (China)			61.2×10^4 (China)			105.3×10^4 (China)		
Annual mean precipitation[a,c]	150–300 (Mongolia)			50–150 (Mongolia)			50–150 (Mongolia)		
(mm yr^{-1})	200–400 (China)			50–200 (China)			20–150 (China)		
Annual mean aridity[c]	2–3 (Mongolia)			4–30 (Mongolia)			3–6 (Mongolia)		
	2–4 (China)			4–40 (China)			5–70 (China)		
Annual mean wind speed[a,c] (m s^{-1})	3–5 (Mongolia)			3–5 (Mongolia)			1–3 (Mongolia)		
	2–4 (China)			3–5 (China)			2–4 (China)		
Dust storm frequency	5–30 (Mongolia)			11–35 (Mongolia)			11–20 (Mongolia)		
(day yr^{-1})[c,d]	5–25 (China)			10–35 (China)			5–35 (China)		
Annual mean dust emission	PM_{10}:	PM_{30}:	PM_{50}:	PM_{10}:	PM_{30}:	PM_{50}:	PM_{10}:	PM_{30}:	PM_{50}:
(10^6 ton yr^{-1})	0.026 (Mon.)	0.037 (Mon.)	0.037 (Mon.)	2.0 (Mon.)	2.9 (Mon.)	8.6 (Mon.)	0.027 (Mon.)	0.041 (Mon.)	0.049 (Mon.)
	0.092 (China)	0.2 (China)	0.5 (China)	2.9 (China)	6.9 (China)	13.2 (China)	5.4 (China)	17.6 (China)	28.9 (China)

[a]Gonggerdaxi (1977);
[b]Murzayev (1958);
[c]Zhao (1994);
[d]Middleton (1991).

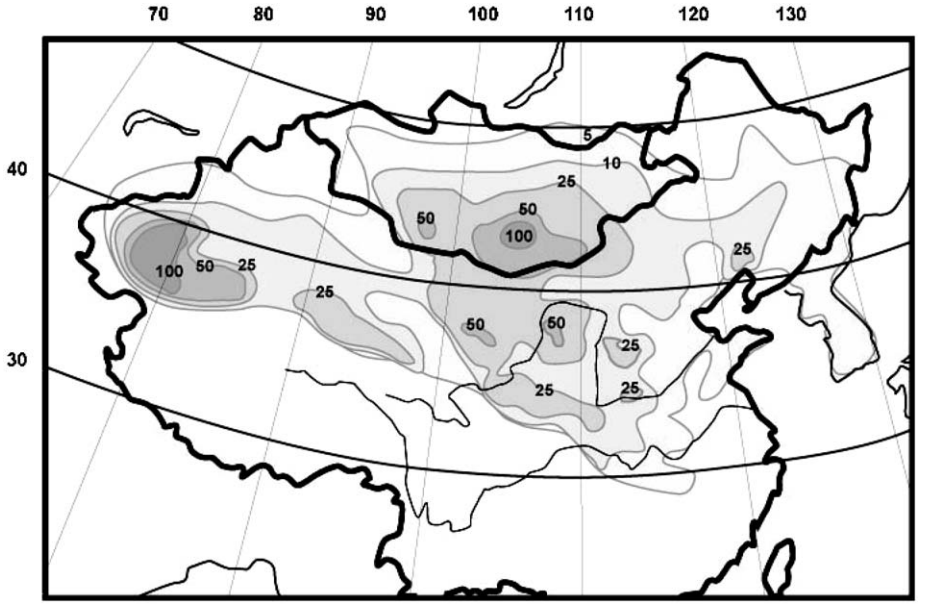

Fig. 6. Dusty days of spring months of 2000–2002 in East Asia.

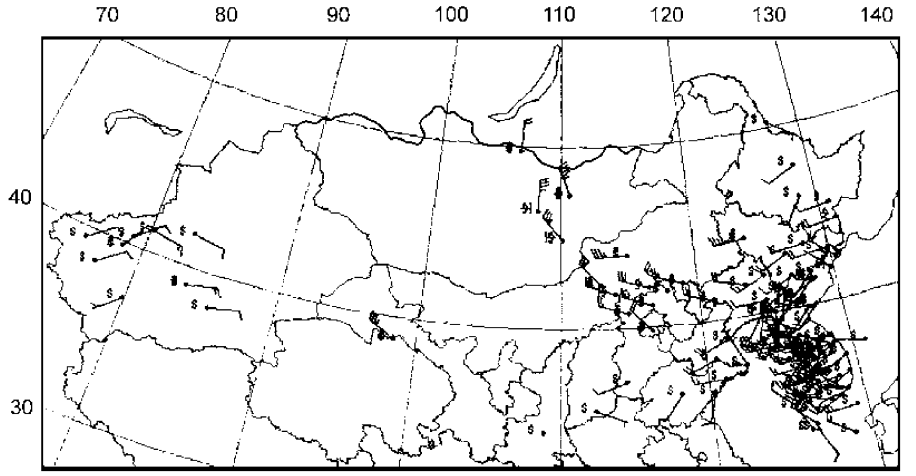

Fig. 7. Surface wind vector field and visibility of 1100 LST 21 March 2002.

Tarim Basin system exhibits a 'concentric (alluvial) distribution pattern'—an outer loop of mountains and an inner loop of gobis surround the central deserts, viz., the Taklimakan Desert (in the Tarim Basin) and the Gurbantunggut Desert (in the Junggar Basin). Because the surrounding mountains modify the surface wind field and limit dust storm transport, no large area of loess deposit exists inside or downwind of the Tarim Basin system (Zhao, 1985).

In the Mongolian Plateau system and downwind vicinity, from northwest to southeast, the surface soil texture shows a coarse-to-fine trend: gobi gravel becomes desert sand, followed by silt and clay of the Loess Plateau. There is no such kind of variation in the Tarim Basin system where the soil texture is finer: the surface sand content of the Taklimakan Desert is 81% while it is 96–99% in the deserts on the Mongolian Plateau and its south extension (Zhao, 1985).

The climate is extremely dry in both dust source systems. The precipitation in the east part of the Mongolian Plateau system is around 300 mm yr^{-1} and rapidly decreases from east to west down to 50 mm yr^{-1} or less in the gobi area. The precipitation in the middle Taklimakan Desert is estimated to be less than

20 mm yr^{-1} (Zhao, 1994). A cold front passage in spring produces strong surface wind in both systems. Because of the difference in topography, northwest wind and northeast wind respectively prevail in the Mongolian Plateau system and the Tarim Basin system. The flat topography in the Mongolian Plateau system also makes the surface wind speed stronger (Zhao, 1994). The finer surface soil texture in the Tarim Basin system makes severe dust storms occur more easily, even a 7–9 m s^{-1} surface wind speed is able to produce severe dust storms (Xu, 1997). Generally, severe dust storms occur with a wind speed of >20 m s^{-1} on the Mongolian Plateau, while it is >17 m s^{-1} in the Taklimakan Desert (Qian et al., 1997).

4.4. Dust storm meteorology—synoptic background and transport route

The cold front passage in spring has been recognized to be the synoptic background of dust storms in East Asia (Chen and Chen, 1987; Xu et al., 1997; Qian et al., 1997; Sun et al., 2001). Typically, the cold front moves southeast, behind which a high-pressure center of cold air passes over the north part of the Tarim Basin system (Fig. 8). Two low-pressure patterns, the 'Warm Low' over the Taklimakan Desert (Xu, 1997) and the 'Mongolian Cyclonic Depression' or 'Cold Vortex' over the Mongolian Plateau (Sun et al., 2001), are often observed. Both kinds of low-level convergence lift dust up to a few kilometers so as to form the long distance transport of dust plumes. The role of the Mongolian Cyclonic Depression has been well recognized and successfully simulated (Uno et al., 2001; Shao, 2002). The high-level transport route of M type dust storms (in the Mongolian Plateau system) is roughly eastward, similar to the near-surface southeastward route. The elevated dust plume sequentially passes over the Manchurian Plain, Korean Peninsula, and Japan Islands, then over the Pacific Ocean, and finally lands on North America. Because of the rarity of weather stations in the huge Taklimakan Desert and nearby mountain area, the Warm Low has not been as well documented as the Mongolian Depression. The near-surface transport of S type dust storms (in the Tarim Basin system) is limited locally and the route of the high-level transport is still lacking research though an eastward route was once supposed. Only Sun et al. (2001) have proposed a 'north-then-east' high-level transport route—namely, the Taklimakan dust is first lifted to a high elevation then transported north and northwest, over Lake Balkhash, before turning east at 50°N by the westerly jet stream. The behavior of the Warm Low and the high-level transport route for the Tarim Basin system deserve further study if only one considers the enormous amount of Takliman dust emitted into the air each year.

The total dust emission from sources in East Asia is estimated to be 10.4×10^6 ton yr^{-1} for PM_{10}, 27.6×10^6 ton yr^{-1} for PM_{30}, and 51.3×10^6 ton yr^{-1} for PM_{50}. The Tarim Basin dust source system contributes slightly more than the Mongolian Plateau dust source system. Some comparative characteristics of the two source systems are briefly listed in Table 3.

5. Summary

(1) In a multidisciplinary study of dust sources in East Asia, the characteristics of dust sources with regard to climate, dust storm meteorology, soil texture, topography, morphology, palaeogeography, and dust emission rate are generally discussed, and a set of five criteria for

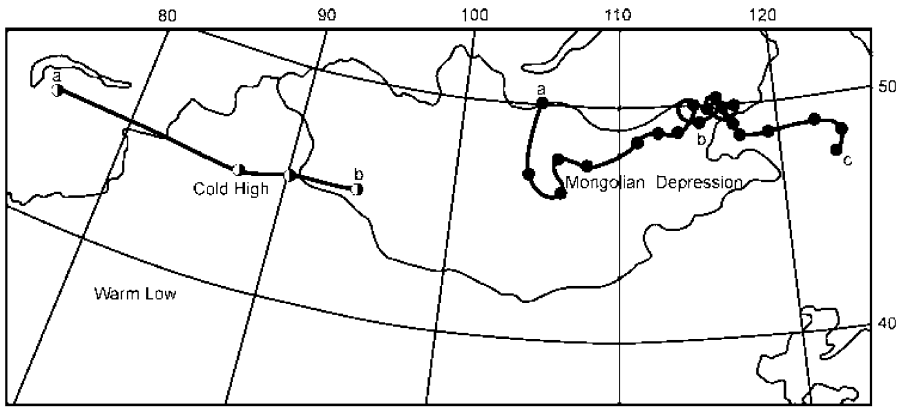

Fig. 8. Surface development of a synoptic system of the 18–22 March 2002 dust storm event. Cold High center: (a) 0800 LST 19 March, (b) 0200 LST 20 March, with a time interval of 6 h. Mongolian Depression center: (a) 0500 LST 19 March, (b) 0800 LST 20 March, (c) 1400 LST 21 March, with a time interval of 3 h. Warm Low: (o) 1400 LST 18 March.

Table 3
Comparative characteristics of the two dust source systems in East Asia

Category	Mongolian Plateau dust source system	Tarim Basin dust source system
Source types in Fig. 5 and Table 2	Chinese Types 1,2 and Mongolian Types 1, 2, and 3	Chinese Type 3
Topography	Plateau, except for Great Lake Basin and Hexi Corridor; Elevation of 500–1800 m	Basin; Elevation of 300–1200 m, except for Tsaidam Basin
Morphology (distribution pattern of gobis and deserts, with or without loess lands)	Linear (aeolian) distribution: gobis, deserts, and loess lands lying in order of northwest to southeast	Concentric (alluvial) distribution: outer loop of mountains and inner loop of gobis surrounding central deserts, with no large loess lands
Surface soil texture	Sand content in desert surface: 96–99%; Particle size decreasing from northwest to southeast	Sand content in desert surface: 81% (Taklimakan Desert)
Annual precipitation, mm yr^{-1}	50–400	20–100
Annual aridity	2–40	10–70
Annual surface wind speed, m s^{-1}	2–6	2–4
Prevailing surface wind direction in spring	Northwest	Northeast
Dusty days of spring 2000–2002 (visibility < 10 km), day	10–100 and up	10–100, and up
Annual frequency of dust storms (visibility < 1 km), day yr^{-1}	5–35	5–35
Typical dust storm type	M (moving) type	S (stationary) type
Synoptic background of dust storms	Cold front passage	Cold front passage
Low-level convergence	Mongolian Cyclonic Depression	Warm Low
Near-surface transport route	Southeastward	Local
High-level transport route	Eastward: passing over Manchurian Plain or North-China Plain, Korean Peninsula, Japan Islands, and Pacific Ocean	North-then-eastward: passing over Tianshan Mountain and Lake Balkhash, reaching 50°N before turning eastward
Annual dust emission, 10^6 ton yr^{-1} (percentage of total emission in East Asia)	PM_{10}: 5.0 (48%) PM_{30}: 10.0 (36%) PM_{50}: 22.4 (44%)	PM_{10}: 5.4 (52%) PM_{30}: 17.6 (64%) PM_{50}: 28.9 (56%)

source identification is developed based on a discussion of the dust emission mechanism.

(2) Like in Northern China, dust sources in Southern Mongolia are classified into three types: (i) Type 1: deserts in dry agricultural areas (south part of East Mongolia Plain), (ii) Type 2: gobi-deserts on flat plateaus (the vast gobi area in south Mongolia), and (iii) Type 3: deserts and gobi-deserts in topographical lows (Great Lake Basin).

(3) The dust emission rate increases from north to south across Mongolia by five orders, with the maximum appearing in the southwest of the gobi area. The total dust emission of Mongolian sources is estimated to be 2.0×10^6 ton yr^{-1} for PM_{10}, 2.9×10^6 ton yr^{-1} for PM_{30}, and 8.7×10^6 ton yr^{-1} for PM_{50}. Type 2 sources contribute 97% to the total annual emission.

(4) The dust source region in East Asia covers Southern Mongolia and Northern China, consisting of the following two parts: (i) Mongolian Plateau dust source system, including deserts and gobi-deserts on the Mongolian Plateau and its southern extension—the Ordos Plateau and Alxa Plateau; and (ii) Tarim Basin dust source system, including deserts and gobi-deserts in the Tarim Basin, Junggar Basin, and east vicinity.

(5) The two source systems are not only related but also distinguished by the topography and distribution pattern of gobis and deserts (with or without loess lands)—namely, a linear (aeolian) distribution pattern for the Mongolian Plateau system and a concentric (alluvial) distribution pattern for the Tarim Basin system. Other environmental characteristics are also discussed, e.g.: M (moving) type dust storms occur in the Mongolian Plateau system while S (stationary) type dust

storms in the Tarim Basin system, in connection with the dust lifting mechanism and long-distance transport routes.

Acknowledgement

We are grateful to Ms. Bonnie Wang for drawing the figures and Mr. Darren Paul Griffith for polishing the English writing of our manuscript.

References

Alfaro, S.C., Rajot, J.L., Lafon, S., Maille, M., Gaudichet, A., 2003. Does soil composition have an influence on the sandblasting process? In: Proceedings of the 2nd International Workshop on Mineral Dust, September 10–12, Paris, France.

Amante-Orozco, A., zobeck, T., 2002. Clay and carbonate effect on fine dust emissions as generated in a wind tunnel. Proceedings of the ICAR5/GCTE-SEN Joint Meeting, 22–25 July, 2002, Lubbock, TX, pp. 79–82.

Bagnold, R.A., 1941. The Physics of Blown Sand and Desert Dunes. Methuen, London.

Chao, S., 1984. The sandy deserts and gobi of China. In: Farouk, E. (Ed.), Deserts and Arid Lands. Martinus Nijhoff Publishers, Boston.

Chen, G., Chen, H., 1987. Study on large-scale feature of duststorm system in East Asia. Papers in Meteorological Research, Publication of The Meteorology Society of Republic of China 10 (1), 57–80.

CMA (China Meteorological Administration), 1970. Mongolian Climate. (Internal publication).

CMA, 2002. Special News Issuing Meeting on Dust Storm Monitoring Network. (March 17, 2002), Beijing.

Cowherd, C., Bohn, Jr. R., Cuscino, T., 1979. Iron and steel plant open source fugitive emission evaluation. EPA-600/2-79-103.

Ding, Y., Wang, S., 2001. Introduction of Climate and Eco-environment in North-west China. (China) Meteorological Press, Beijing.

Gillette, D., 1979. Environmental factors affecting dust emission by wind erosion. In: Morales, C. (Ed.), Saharan Dust. Wiley, New York, pp. 71–94.

Gillette, D., 1983. Threshold velocities for wind erosion on natural terrestrial arid surfaces. In: Pruppacher, H. (Ed.), Precipitation Scavenging, Dry Deposition and Resuspension. Elsevier, New York.

Ginoux, P., Chin, M., Tegen, I., Prospero, J., Holben, B., Dubovik, O., Lin, S., 2001. Sources and distributions of dust aerosols simulated with the GOCART model. Journal of Geophysical Research 106, 20255–20273.

Gonggerdaxi, B., 1977. Mongolian Economic Geography. Liaoning People Press, Beijing.

Goudie, A.S., Middleton, N.J., 2001. Saharan dust storms: nature and consequences. Earth-Science Reviews 56, 179–204.

Harpet, R.J., Gilkes, R.J., Hill, M., Carter, D.J., 2002. The incidence of wind erosion as related to soil properties and geomorphic history in south-western Australia. Proceedings of the ICAR5/GCTE-SEN Joint Meeting, 22–25 July, 2002, Lubbock, Texas, pp. 158–162.

Iversen, J., 2002. Simulated atmospheric vortex threshold. Proceedings of the ICAR5/GCTE-SEN Joint Meeting, 22–25 July, 2002, Lubbock, Texas, pp. 111–112.

Joussaume, S., 1990. Three dimensional simulations of the atmospheric cycle of desert dust particles using a general circulation model. Journal of Geophysical Research 95, 1909–1941.

Jutze, G., Axetell, K., 1976. Factors influencing emissions from fugitive dust. Symposium on Fugitive Emission Measurement and Control (May 1976, Hartford, CT). EPA technical report: EPA-600/2-76-246.

Liao, K. (Ed.), 1999. National Physical Atlas of China. Cartographic Publishing House, Beijing.

Littmann, T., 1991. Dust storm frequency in Asia: climatic control and variability. International Journal of Climatology 11, 393–412.

Mahowald, N., Kohfeld, K., Hansson, M., Balkanski, Y., Harrison, S., Prentice, I.C., Schulz, M., Rodhe, H., 1999. Dust sources and deposition during the last glacial maximum and current climate: a comparison of model results with paleodata from ice cores and marine sediments. Journal of Geophysical Research 104, 15895–15916.

Marticorena, B., Bergametti, G., 1995. Modeling the atmospheric dust cycle: 1. Design of a soil-derived dust emission scheme. Journal of Geophysical Research 100, 16415–16430.

Middleton, N., 1991. Dust storms in the Mongolian People's Republic. Journal of Arid Environments 20, 287–297.

Murzayev, E., 1958. Mongolian People's Republic (Natural Geography). Triple Press, Beijing.

Natsagdorj, L., Jugder, D., Chung, Y.S., 2003. Analysis of dust storms observed in Mongolia during 1937–1999. Atmospheric Environment 37, 1401–1411.

Nickling, W.G., Gillies, J.A., 2003. The role of shear stress partitioning on dust emission. In: Proceedings of the 2nd International Workshop on Mineral Dust. September 10–12, Paris, France.

OAQPS (EPA), 1977. Guideline for Development of Control Strategies in Areas with Fugitive Dust Problems. EPA-405/2-77-029.

Pisparov, H., 1959. Mongolian Soils. Science Press, Beijing.

Prospero, J., Ginoux, P., Torres, O., Nicholson, S., Gill, T., 2002. Environmental characterization of global sources of atmospheric soil dust derived from the NIMBUS-7 Total Ozone Mapping Spectrometer (TOMS) absorbing aerosol product. Reviews of Geophysics 40 (1), 1002,.

Qian, Z., He, H., Qu, Z., Chen, M., 1997. Standardization of dust storms in North-west of China and statistical characterization of the dust storms. In: Fang, Z. (Ed): Studying of Chinese Dust Storms, pp. 1–10.

Shao, Y., 2002. Numerical simulation of Northeast Asian dust storms using an integrated wind erosion modeling system. Journal of Geophysical Research 107 (D24), 4814.

Shao, Y., Raupach, M.R., Findlater, P.A., 1993. The effect of saltation bombardment on the entrainment of dust by wind. Journal of Geophysical Research 98, 12719–12726.

Sun, J., Liu, T., Lei, Z., 2000. Sources of heavy dust fall in Beijing, China on April 16, 1998. Geophysical Research Letters 27 (14), 2105–2108.

Sun, J., Zhang, M., Liu, T., 2001. Spatial and temporal characteristics of dust storms in China and its surrounding regions, 1960–1999: relations to source area and climate. Journal of Geophysical Research 106 (D10), 10325–10333.

Tegen, I., Fung, I., 1994. Modeling of mineral dust in the atmosphere: sources, transport, and optical thickness. Journal of Geophysical Research 99, 22897–22914.

Tuvdendorzh, D., 1974. The dust storms of the territory of Mongolian People's Republic. See quotation in Middleton (1991).

Uno, I., Amano, H., Emori, S., Kinoshita, N., Matsu, I., Sugimoto, N., 2001. Trans-Pacific yellow sand transport observed in April 1998: a numerical simulation. Journal of Geophysical Research 106, 18331–18344.

Xiong, Y., Li, Q., 1990. Soil of China. Science Press, Beijing.

Xu, B., Qian, Z., Jiao, Y., 1997. Comprehensive analyses of synoptic fields and forecast of five severe dust storms in North-west China. In: Fang, Z., et al. (Eds.), Studying of Chinese Dust Storms, pp. 44–51.

Xu, Q., Hu, J., 1996. Spatial distribution and seasonal variation of dust storms in North-west China. Quarterly Journal of Applied Meteorology 7, 479–482.

Xu, X., 1997. Satellite image analyses and studying of dust storms in the Tarim Basin. In: Fang, Z., et al. (Eds.), Studying of Chinese Dust Storms, pp. 88–91.

Xuan, J., 1999. Dust emission factors for environment of Northern China. Atmospheric Environment 33, 1767–1776.

Xuan, J., Sokolik, I., 2002. Characterization of Sources and Emission Rates of Mineral Dust in Northern China. Atmospheric Environment 36, 4863–4876.

Xuan, J., Liu, G., Du, K., 2000. Dust emission inventory in Northern China. Atmospheric Environment 34, 4565–4570.

Yi, Y., Okumura Takenobu, Sueyasu Katsumi, Kamichika Makio, 2002. The formation and stability of surface armoring by coarse sand particles. Proceedings of the ICAR5/GCTE-SEN Joint Meeting, 22–25 July, 2002, Lubbock, Texas, pp. 70–73.

Zender, C.S., Newman, D., 2002. Simulated global atmospheric dust distribution: sensitivity to regional topography, geomorphology, and hydrology. Proceedings of the ICAR5/GCTE-SEN Joint Meeting, 22–25 July, 2002, Lubbock, Texas, pp. 304–307.

Zhang, T. (Ed.), 1999. Loess Plateau. Science Press, Beijing.

Zhao, S., 1985. Physical Geography of China Arid Lands. Science Press, Beijing,, pp. 1–17.

Zhao, G. (Ed.), 1994. Atlas of Climate Resources of China. Cartographic Publishing House, Beijing.

Zobec, T.M., Van Pelt, R.S., Kjelgaard, J., Sharratt, B., 2003. Linkage of saltation and dust emission in bare agricultural fields. In: Proceedings of the 2nd International Workshop on Mineral Dust, September 10–12, Paris, France.